

PAPER • OPEN ACCESS

Optimal operation of RSOC integrated energy systems considering multi-state transitions

To cite this article: Xuzheng Zhang *et al* 2022 *J. Phys.: Conf. Ser.* **2404** 012023

View the [article online](#) for updates and enhancements.

You may also like

- [Rashba coupling and spin switching through surface states of Dirac semimetals](#)
Yuriko Baba, Francisco Domínguez-Adame, Gloria Platero *et al.*
- [Identifying the graphene *d*-wave superconducting symmetry by an anomalous splitting zero-bias conductance peak](#)
Chuan-Shuai Huang, Yang Yang, Y C Tao *et al.*
- [Spin polarization and Fano–Rashba resonance in nonmagnetic graphene](#)
Wei-Tao Lu and Qing-Feng Sun



ECS
The
Electrochemical
Society
Advancing solid state &
electrochemical science & technology

DISCOVER
how sustainability
intersects with
electrochemistry & solid
state science research

Optimal operation of RSOC integrated energy systems considering multi-state transitions

Xuzheng Zhang¹, Haoyu Yu¹, Hongfei Zhao¹, Zihang Zhang¹, Kai Wu¹ and Jun Zhou^{1*}

¹ School of Electrical Engineering, Xi'an Jiaotong University, Xi'an, Shaanxi, 710049, China

*Corresponding author's e-mail: zhoujun@mail.xjtu.edu.cn

Abstract. Reversible solid oxide fuel cells (RSOC) can realize energy storage and power generation in a compact structure, and their high-temperature operation characteristics provide the possibility for combined heat and power generation. Therefore, RSOC can be used as the node of the multi-energy flow intersection of the integrated energy system. The flexible operation mode of RSOC will greatly reduce the operation cost. However, the optimal operation of an integrated energy system including RSOC is very rare at present, so this paper establishes an integrated energy system of the electric gas network including RSOC. On this basis, this paper constructs an RSOC model, a DC power flow model and a linearized gas power flow model considering multiple operating states. Then, based on GAMS, the economic cost of a 24-20 electric gas composite network is optimized. After verifying the reliability of the model, the optimization results considering two working conditions and four working conditions are compared. It is concluded that the model considering multiple operating states of RSOC will reduce the operating cost of the system by 24%.

1. Introduction

At present, global greenhouse gas emissions are excessive, and the energy crisis is gradually approaching. And the goal of achieving carbon neutrality by 2060 was raised. Therefore, China must adjust its energy consumption structure ^[1]. In the field of power, the fundamental way to achieve carbon neutrality is to gradually reduce the proportion of thermal power and increase new energy penetration. However, the instability of new energy will reduce the stability of the electricity supply. Using the interconnection and complementarity of various energy sources and cooperating with energy storage can increase the penetration of new energy and ensure the safety of the energy supply. Reversible solid oxide cells (RSOC) can realize hydrogen energy storage and power generation at the same time, and can be used as the core device to connect multiple types of energy ^[3]. Therefore, the research on the optimal operation of the electricity-gas integrated energy system with RSOC is of forward-looking and important significance for energy conservation and emission reduction.

Using RSOC to electrolyze water to produce hydrogen is a relatively advanced technology. Firstly, RSOC can realize energy storage and power generation in one piece of equipment ^[4]. Secondly, RSOC has a full solid-state structure and has a good application prospect as an electrolytic station, cogeneration power station, emergency standby power supply, distributed power supply, etc. Besides, RSOC works at high temperatures, and the working temperature is 700°C~1000°C, it is easy to carry out cogeneration and improve economic benefits. ^[5]



RSOC can integrate various energy flows, which greatly enhances the coupling between different energy sources and improve the operational flexibility and economy of the system. However, at present, most integrated energy systems are based on separate fuel cells or two parts of fuel cells and electrolytic cells, and there is little research on the optimal design of integrated energy systems based on RSOC. Literature [6] takes RSOC as the energy node to establish the capacity optimization model of an integrated energy system with the lowest energy cost and obtains the optimal capacity and optimal scheduling strategy, which shows that the integrated energy system including RSOC can significantly reduce the energy cost. Yang [7] proposed a novel method and mathematical model for wind power and RSOC to participate in the power market, and the research mainly focuses on the planning and operation of the network. RSOC is usually assumed to be an input-output component with fixed conversion efficiency [8]. However, the flexibility of the electrolyzer is mainly reflected in the nonlinear partial load characteristics of RSOC, the switching of different states of RSOC and the starting time of different states, standby loss and ramp rate [9]. According to the different initial states of start-up, the start-up process can be further divided into cold start-up and hot start-up. G. Matute developed a multi-state economic model for the optimal operation of an electric hydrogen production system. Based on this model, the optimal scheduling problem of the electrolyzer is expressed as a mixed integer nonlinear programming. They tested the model with real data and compared it with a simple model with only two states. The results show that the multi-state model can reduce production cost [10]. However, there is still no optimal operation model for electric gas-integrated energy systems including multi-state RSOC.

Based on the above background, this paper develops a multi-state RSOC model, which describes the four states of RSOC including power generation mode, electrolysis mode, shutdown mode and hot standby mode. On this basis, a 24-20 node electricity gas-integrated energy system including RSOC is constructed for optimal operation.

2. System structure and operation mode

2.1. System structure

Taking RSOC as the energy node, this paper constructs an electricity-gas-integrated energy network, as shown in Figure 1. The network includes a power network, hydrogen network and natural gas pipeline network. When wind power generation is redundant, RSOC can convert excess wind power into hydrogen and store it in natural gas pipelines. During the peak period of power consumption, RSOC works in the power generation mode to burn fuel gas and generate electric energy, improving the penetration rate of new energy. In addition, injecting hydrogen and natural gas into the natural gas pipeline can not only reduce the energy storage cost of hydrogen, but also transport it to gas users.

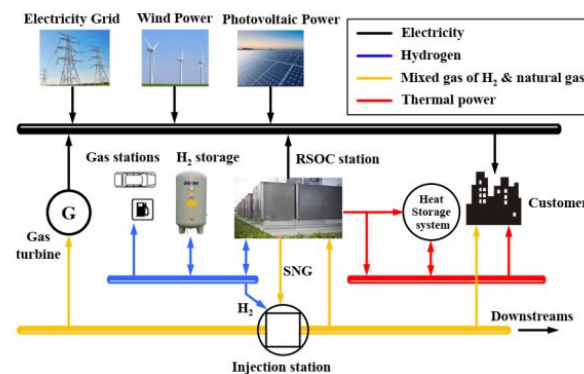


Figure 1. Integrated energy system considering various operating states of RSOC

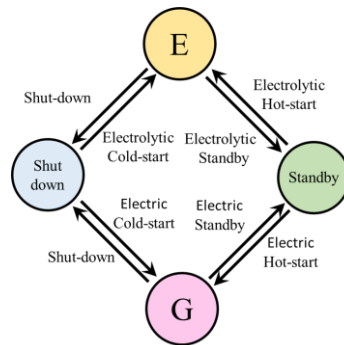


Figure 2. Schematic diagram of state transition of RSOC

2.2. Operation mode of RSOC

As the conversion hub of different energy flows in the integrated energy system, the choice of its operation mode has a great impact on the flexibility of the scheduling of the integrated energy system. Therefore, this paper establishes the RSOC operation model including power generation mode, electrolysis mode, shutdown mode, and hot standby mode. In the hot standby mode, RSOC will neither generate electricity nor generate hydrogen, but maintain the pressure and temperature inside RSOC unchanged for rapid start-up. In the shutdown mode, the RSOC unit does not work at all, and the temperature and air pressure inside the system are no longer maintained. The state transition diagram of RSOC is shown in Figure 2.

3. Mathematical models

3.1. Objective function

The objective function of the system is to meet the load demand of customers and minimize the operation cost at the same time. The optimization equation is shown in formula (1), which includes: 1) the cost of thermal power generation; 2) The cost of natural gas purchased from the gas source node; 3) The cost of wind cuts; 4) Cold start and hot start costs.

$$C = \sum_{g \in \Omega T, t} b_g P_{g,t} + \sum_{n,t} C_n Sg_{n,t} + \sum_{i,t} VOLW \times P_{i,t}^{wc} + \sum_{g \in \Omega_r, t} \left(C^{HS} (Y_{r,t-1}^{gen} + Y_{r,t-1}^{ele}) + C^{CS} (Z_{r,t-1}^{gen} + Z_{r,t-1}^{ele}) \right) \quad (1)$$

Where, g represents all generator sets including RSOC; r represents the RSOC unit set, $r \in g$; n represents the set of all gas injection nodes; i represents all grid node sets. b_g , C_g , $VOLL$, $VOLW$ and b_g are power purchase price, natural gas price, penalty price for not supplied load, penalty price for wind abandonment and RSOC heating price respectively; $P_{g,t}$, $Sg_{n,t}$, $LS_{i,t}$, $P_{i,t}^{wc}$ and $H_{g,t}$ refer to the main network power purchase, gas purchase, unsupplied load, system waste air volume and heating energy required by RSOC at each time.

3.2. RSOC operation model

3.2.1. Part-load operation model.

The partial load characteristics of RSOC in this work are described by the fitting curve of power generation and electrolysis characteristics under a steady state, and the curve is shown in Figure 3. The specific function relation is obtained by the incremental linearization method. The partial load description formula considering multiple states in SOFC mode is shown in formula (2). formula (2) includes three relaxation variables: χ_{1t} , χ_{2t} , and χ_{3t} . This is because the power generation input-output relationship is only applicable to the power generation mode, and this constraint must be released in the hot standby state, shutdown state, and electrolytic state. χ_{1t} , χ_{2t} , and χ_{3t} are 0 under

power generation mode, and large enough or small enough in the other three states. Equation (6) is a partial load formula considering multiple states in SOEC mode. Equation (7) shows that the proportion of the maximum SNG output is. Equation (8) represents the energy lost in the CO₂ preheating and capture process.

$$P_{r,t} = f(E_{r,t}^{in}) + \chi_{1t} + \chi_{2t} + \chi_{3t} \quad (2)$$

$$-MU_{r,t}^s \leq \chi_{1t} \leq MU_{r,t}^s \quad (3)$$

$$-MU_{r,t}^i \leq \chi_{2t} \leq MU_{r,t}^i \quad (4)$$

$$-MU_{r,t}^e \leq \chi_{3t} \leq MU_{r,t}^e \quad (5)$$

$$E_{r,t}^{H_2} + \chi E_{r,t}^{SNG} = F(P_{r,t}^{P2G}) + \gamma_{1t} + \gamma_{2t} + \gamma_{3t} \quad (6)$$

$$\frac{E_{r,t}^{SNG}}{H_{NG}} \leq \beta \left(\frac{E_{r,t}^{SNG}}{H_{NG}} + \frac{E_{r,t}^{H_2}}{H_{H_2}} \right) \quad (7)$$

$$E_{r,t}^{CO_2} = \eta^{CO_2} E_{r,t}^{SNG} \quad (8)$$

Where, $E_{r,t}^{in}$ is the fuel intake; $P_{r,t}$ is the generating capacity; $P_{r,t}^{P2G}$ is the power consumption for P2G; $E_{r,t}^{H_2}$, $E_{r,t}^{SNG}$ are the amount of hydrogen and SNG injected into the natural gas pipeline network respectively, and it is assumed that the effect of SNG yield fraction on electrolysis efficiency is linear.

3.2.2. Operation schedule model.

RSOC units can be regarded as thermal units with various states. Therefore, in this paper, four 0-1 variables are used to represent the operating state of RSOC, and six 0-1 variables are used to represent the conversion action of RSOC. Equations (9) to (13) are equations describing the operating state and on-off action of RSOC; Equations (14) to (16) represent the Minimum switching interval. Equation (9) represents that the RSOC unit can only work in the hot standby state, shutdown state, power generation state and electrolysis state; Equation (10) indicates that the unit cannot be directly converted from shutdown state to hot standby state.

$$U_{r,t}^{gen} + U_{r,t}^{ele} + U_{r,t}^s + U_{r,t}^i = 1 \quad (9)$$

$$U_{r,t}^s + U_{r,t-1}^i \leq 1 \quad (10)$$

$$\begin{cases} Y_{r,t-1}^{ele} = U_{r,t-1}^s \cdot U_{r,t}^{ele} \\ Y_{r,t-1}^{gen} = U_{r,t-1}^{gen} \cdot U_{r,t}^{gen} \end{cases} \quad (11)$$

$$\begin{cases} Z_{r,t-1}^{ele} = U_{r,t-1}^i \cdot U_{r,t}^{ele} \\ Z_{r,t-1}^{gen} = U_{r,t-1}^i \cdot U_{r,t}^{gen} \end{cases} \quad (12)$$

$$\begin{cases} W_{r,t-1}^{ele} = U_{r,t-1}^{ele} \cdot (U_{r,t}^i + U_{r,t}^s) \\ W_{r,t-1}^{gen} = U_{r,t-1}^{gen} \cdot (U_{r,t}^i + U_{r,t}^s) \end{cases} \quad (13)$$

$$Y_{r,t}^{ele} + Z_{r,t}^{ele} + Y_{r,t}^{gen} + Z_{r,t}^{gen} + \sum_{k=1}^{UTr} (W_{r,t}^{ele} + W_{r,t}^{gen}) \leq 1 \quad (14)$$

$$Y_{r,t}^{ele} + Z_{r,t}^{ele} + Y_{r,t}^{gen} + Z_{r,t}^{gen} + \sum_{k=1}^{UTr} (W_{r,t}^{ele} + W_{r,t}^{gen}) \leq 1 \quad (15)$$

$$W_{r,t}^{ele} + W_{r,t}^{gen} + \sum_{k=1}^{DT_r} (Y_{r,t}^{ele} + Z_{r,t}^{ele} + Y_{r,t}^{gen} + Z_{r,t}^{gen}) \leq 1 \quad (16)$$

Where, $U_{r,t}^{gen}$, $U_{r,t}^{ele}$, $U_{r,t}^s$, $U_{r,t}^i$ represent the unit R of RSOC is in power generation state, electrolysis state, hot standby state and shutdown state at time t ; $Y_{r,t}^{gen}$, $Y_{r,t}^{ele}$, $Z_{r,t}^{gen}$, $Z_{r,t}^{ele}$, $W_{r,t}^{gen}$, and $W_{r,t}^{ele}$ represent the electric starting action, electrolytic hot starting action, power generation cold starting action, electrolytic cold starting action, power generation shutdown action and electrolytic shutdown action of RSOC unit; U_{Tr} and D_{Tr} indicates the minimum time between start-up and shutdown respectively.

There are also climbing restrictions for RSOC units. Equation (17) describes the constraints of RSOC in different states. Equation (19) is the climbing constraint of the equation.

$$U_{r,t}^{gen} P_{\min}^{gen} / sbase + U_{r,t}^s P_s / sbase \leq P_{r,t} \leq U_{r,t}^s P_s / sbase + U_{r,t}^{gen} P_{\max}^{gen} / sbase \quad (17)$$

$$P_{r,t} = P_r^{\min} U_{r,t}^{gen} + P_{r,t}^{op} \quad (18)$$

$$-RD \leq P_{r,t}^{op} - P_{r,t-1}^{op} \leq RU \quad (19)$$

3.3. Electricity network

The power flow constraint of the distribution network adopts the DC power constraint, and the model is composed of Equations (20) ~ (24).

$$\sum_{g \in \Omega_G^i} (P_{g,t} - P_{g,t}^{P2G}) + LS_{i,t} + P_{i,t}^w - L_{i,t} = \sum_{j \in \Omega_j^i} P_{ij,t} \quad (20)$$

$$P_{ij,t} = \frac{\delta_{i,t} - \delta_{j,t}}{X_{ij}} \quad (21)$$

$$-P_{ij}^{\max} \leq P_{ij,t} \leq P_{ij}^{\max} \quad (22)$$

$$P_t^{pw} = P_i^w + P_i^{wc} \quad (23)$$

$$0 \leq LS_{i,t} \leq L_{i,t} \quad (24)$$

Where, $L_{i,t}$ is the electrical load, $\delta_{i,t}$ is the phase angle of node i ; $X_{i,j}$ is the phase angle of the transmission line connecting node i and node j ; $P_{i,t}^j$ is the predicted wind power generation.

3.4. Gas Network

Gas network constraints include upper and lower pressure constraints and gas flow balance constraints. At each gas node, the amount of gas supplied by the gas source, pipeline and P2G shall be equal to the gas consumption of the node. For the convenience of calculation, the volume of injected H_2 is converted into the volume of SNG with the same energy. Equations (25) - (26) represent gas flow constraints and gas purchase constraints; The node pressure constraint follows the Weymouth formula.

$$\sum_m Q_{n,m,t} = \sum_m Q_{m,n,t} + \sum_{r \in \Omega_R^n} \frac{E_{r,t}^{H_2} + E_{r,t}^{SNG}}{H_{NG}} - \sum_{r \in \Omega_R^n} \frac{E_{r,t}^{in} + E_{r,t}^{sl} + E_{r,t}^{CO_2}}{H_{NG}} + Sg_{n,t} - GL_{n,t} \quad (25)$$

$$Sg_n^{\min} \leq Sg_{n,t} \leq Sg_n^{\max} \quad (26)$$

$$Q_{n,m}^{\min} \leq Q_{n,m,t} \leq Q_{n,m}^{\max} \quad (27)$$

$$Q_{m,n,t} |Q_{m,n,t}| = C_{mm}^2 (P_{m,t}^2 - P_{n,t}^2) \quad (28)$$

$$P_n^{\min} \leq P_{n,t} \leq P_n^{\max} \quad (29)$$

4. Case studies

As shown in Figure 3, the tested power natural gas connection energy system network consists of a Belgian 20-node natural gas system and a modified IEEE rts-24 bus power system [11]. In this system, three wind farms with capacities of 750mW, 1250 MW and 1000MW are installed on power buses 1, 19 and 21. In addition to providing electricity, the remaining wind energy can also be used to participate in the P2G process. Four RSOC stations, namely RSOC1, RSOC2, RSOC3 and RSOC4, are installed on buses 1, 2, 16 and 22, with capacities of 152 MW, 152 MW, 155 MW and 300 MW respectively. Figure 4 shows the wind power capacity, power load and gas load data of the system, and considers the wind power penetration levels of 100% and 50%.

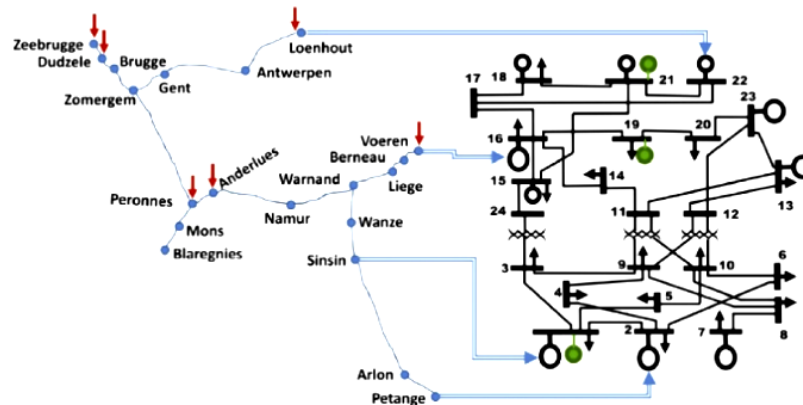


Figure 3. 24-node electricity network and 20-node gas network

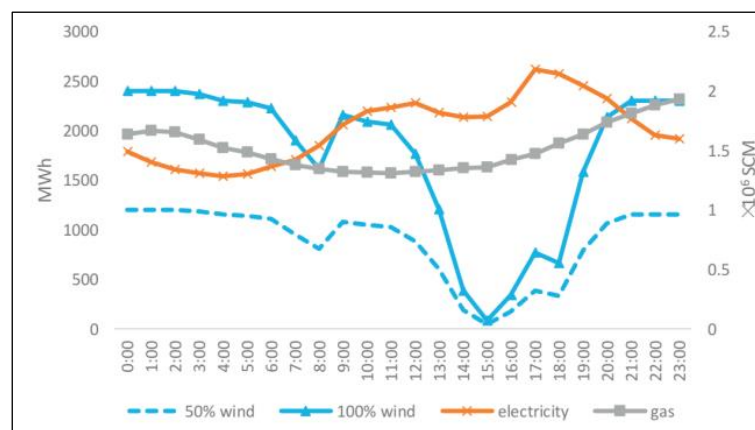


Figure 4. Wind power capacity, power load and the gas load of the system in each time period

The cold start-up cost and hot start-up cost of the four units are shown in Table 1 respectively.

Table 1. Hot start and cold start costs of RSOC

Power unit	Pmax/MW	Cold start cost /\$	Hot start cost /\$
SOC1	152	143.2752	1241.7184
SOC2	152	143.2752	1241.7184
SOC3	155	146.103	1266.226
SOC4	300	282.78	2450.76

5. Numerical results

Using the above model and algorithm, the optimization calculation is carried out in GSMS according to an example, the influence of wind power permeability on the scheduling results is studied, and the economic cost is compared with the model considering only two working conditions.

5.1. Influence of wind power penetration on dispatching results

Figure 5 shows the optimal output of the system under different wind power permeability. In the figure, the level of wind power generation decreases with the reduction of wind power permeability level, and the level of wind abandonment also decreases significantly. During the peak period of power consumption, thermal power generation and SOC power generation increase because of the shortage of wind power generation; Secondly, with the decline of wind power permeability, the time of SOC units working in the electrolytic state is getting shorter and shorter. When the wind power permeability is 30%, SOC units only work in the electrolytic state after 19:00.

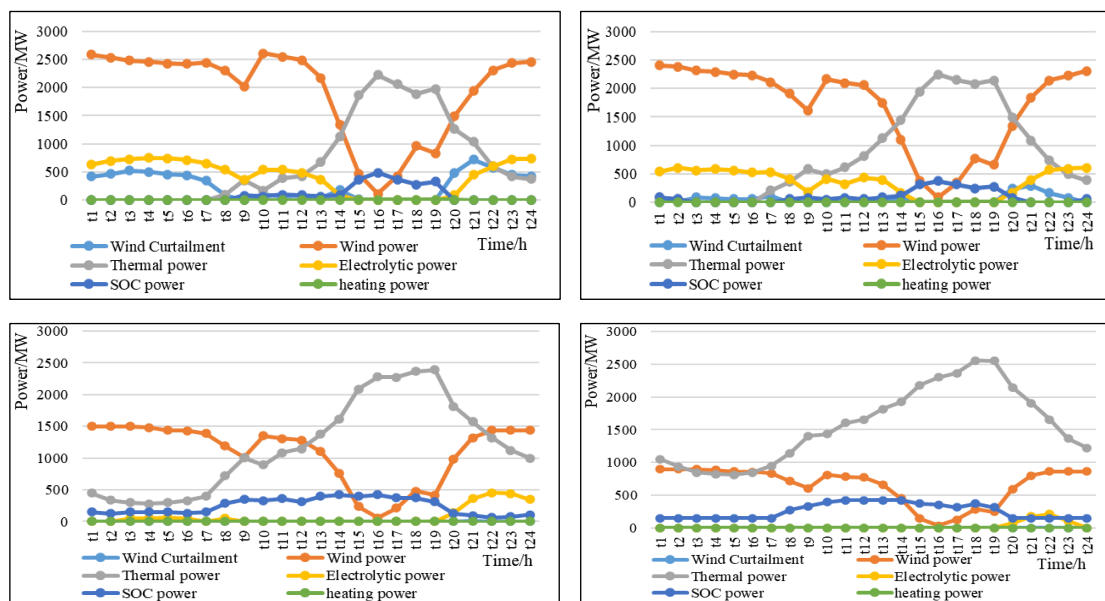


Figure 5. Output of system under wind power permeability of 100% (a), 80% (b), 50% (c) and 30% (d)

Figure 6 shows the output and wind rejection of each unit under different wind power permeability of the system. The point at which the power generation/electrolysis output of the four SOC units is 0 is greatly increased, compared with the procedure under the previous two working conditions. After reviewing the data, it is found that most of the points whose output is 0 are in the hot standby mode. The addition of a hot standby mode is the main reason for the significant decline in operating costs. Secondly, with the decline of wind power permeability, each unit works in the power generation mode become longer, especially unit 2 is in the full load state in 24 hours. Finally, from the change in wind power permeability, the operation result of the system is reasonable.

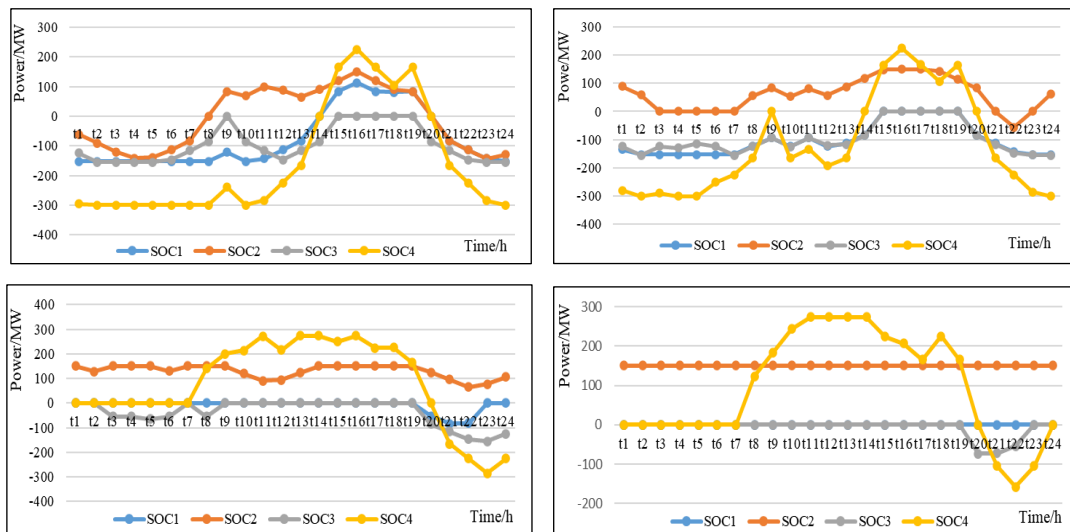


Figure 6. The output of RSOC under wind power permeability of 100%(a), 80%(b), 50%(c) and 30%(d)

5.2. Economic benefit analysis

From Table 2, it can be found that: firstly, at the same level of 100% wind power penetration, the operation cost under the four working conditions is significantly reduced, and the cost is reduced by about 24%. This is because the hot standby mode is added to the level of the original electrolysis and power generation conditions according to the actual situation. Therefore, it only needs to pay a small amount of cost to maintain the SOC air pressure and temperature, which can avoid the high cold start cost and reduce the operation cost. Secondly, with the decline of wind power penetration rate, the operating cost of the system is declining, because, in the case of large wind power capacity, a 100% penetration rate will lead to large-scale wind abandonment, thereby increasing the operating cost. In the process of the wind power penetration rate decreasing from 100% to 80%, the operating cost is greatly reduced. After 80%, the cost reduction is not significant because the waste air volume is very small.

Table 2. Comparison of economic optimization results under different permeability

	100% wind power penetration under two working conditions	100% wind power penetration under four working conditions	80% wind power penetration under four working conditions	50% wind power penetration under four working conditions
EC	414180.6	490795.6	267770.2	232719.9
GC	438338.7	148035.8	119389.6	133666.8
HC	572.0761	196.6511	244.3241	470.7709
SC		1430.88	1567.56	1147.14
cost	853091.4	640459	388971.7	368004.6
pcc	255573.8	319356.4	65662.87	685.9942

6. Conclusion

This work studies the optimal scheduling model of electric gas integrated energy system including the complete RSOC model, which includes the distribution network power flow model, linearized natural gas power flow model, unit combination model considering electrolysis/generation/shutdown/hot standby mode and switching state, and RSOC stack model considering various working conditions, thus forming a MILP problem. In the case of 24-20 nodes, the scheduling of RSOC under different wind power permeability is researched to verify the reliability of the model. And compared with the RSOC operation mode considering only two working modes, it is proved that the operation strategy considering the switching of multiple working conditions can increase the flexibility of scheduling and reduce the operation cost by about 24%. Through the analysis of operation loading and cost

composition, we find that the addition of a hot standby state is the main reason to reduce the cost of the integrated energy system including RSOC.

Acknowledgments

Financial support from the National Natural Science Foundation of China (NSFC) (Project numbers: 51737011 and 51877173).

References

- [1] Zhao T, Wu W, Gao Y. (2022) Power system supply and demand planning to realize carbon cycle under the goal of carbon neutralization. *Power System Technology*:1-13
- [2] Zhang ZG, Kang CQ. (2022) Challenges and Prospects for Constructing the New-type Power System Towards a Carbon Neutrality Future. *Proceedings of the CSEE*, 42(08):2806-2819.
- [3] Zhang ZH, Zhou Jun, Zong Z, et al. (2019) Development of a Novel Energy System Based on Reversible Solid Oxide Cells and Power to Gas Technology for the Urban Energy Conversion and Storage. *ECS Transactions*, 91(1): 2771-2781.
- [4] Christopher H. Wendel et al. Modeling and experimental performance of an intermediate temperature reversible solid oxide cell for high-efficiency, distributed-scale electrical energy storage. *Journal of Power Sources*, 2015, 283: 329-342.
- [5] Barelli L, Bidini G, Gallorini F, et al. (2013) Design optimization of a SOFC-based CHP system through dynamic analysis. *International Journal of Hydrogen Energy*, 38(1): 354-369.
- [6] Ren N, Jingya W, Zonglei X. (2018) Research on capacity matching optimization and scheduling of multi-energy flow distributed integrated energy system. *Grid Technology*, 42(11):3504-3512.
- [7] Zijuan Y. (2020) Research on key technologies for economic evaluation and operation optimization of energy conversion based on electricity-to-gas. Southeast University.
- [8] Zeng Q, Fang J, Li J, Chen Z. (2016) Steady-state analysis of the integrated natural gas and electric power system with bi-directional energy conversion. *Applied Energy*, 184:1483–1492.
- [9] Buttler A, Spliethoff H. (2018) Current status of water electrolysis for energy storage, grid balancing and sector coupling via power-to-gas and power-to-liquids: A review. *Renewable & Sustainable Energy Reviews*, 82: 2440-2454.
- [10] Matute, G, Yusta JM, Beyza J, et al. (2020) Multi-state techno-economic model for optimal dispatch of grid connected hydrogen electrolysis systems operating under dynamic conditions. *International Journal of Hydrogen Energy*, 46(2).
- [11] Soroudi A. (2017) *Power system optimization modeling in GAMS*. Springer International Publishing AG, Switzerland.
- [12] Carrion M, Arroyo JM. (2006) A computationally efficient mixed-integer linear formulation for the thermal unit commitment problem. *IEEE Trans Power System*, 21(3):1371-8.